

Interaction-induced Fermi-surface renormalization in the t_1 - t_2 Hubbard model close to the Mott-Hubbard transition

Luca F. Tocchio,¹ Federico Becca,² and Claudius Gros¹¹*Institute for Theoretical Physics, Frankfurt University, Max-von-Laue-Straße 1, D-60438 Frankfurt a.M., Germany*²*CNR-IOM-Democritos National Simulation Centre and International School for Advanced Studies (SISSA), Via Beirut 2, I-34151 Trieste, Italy*

(Received 20 January 2010; revised manuscript received 16 April 2010; published 11 May 2010)

We investigate the nature of the interaction-driven Mott-Hubbard transition of the half-filled t_1 - t_2 Hubbard model in one dimension, using a full-fledged variational Monte Carlo approach including a distance-dependent Jastrow factor and backflow correlations. We present data for the evolution of the magnetic properties across the Mott-Hubbard transition and on the commensurate to incommensurate transition in the insulating state. Analyzing renormalized excitation spectra, we find that the Fermi surface renormalizes to perfect nesting right at the Mott-Hubbard transition in the insulating state, with a first-order reorganization when crossing into the conducting state.

DOI: [10.1103/PhysRevB.81.205109](https://doi.org/10.1103/PhysRevB.81.205109)

PACS number(s): 71.27.+a, 71.10.Fd, 71.30.+h, 75.10.Jm

I. INTRODUCTION

Low-dimensional Fermi gases and insulators with intermediate and strong couplings show a plethora of interesting phenomena, both in the domains of synthesizable materials¹ and of ultracold atom gases,² with the proximity of metallic, magnetic, superconducting, and insulating phases being a key target for experimental and theoretical studies. One-dimensional correlated electron systems are hence good targets, to give an example, for the exploration of photoinduced phase transitions,³ having in part extremely large third-order nonlinear optical susceptibilities, with possible applications to all-optical switching devices.⁴

Here, we are interested in the nature of the interaction-driven Mott-Hubbard transition which occurs in the one-dimensional t_1 - t_2 Hubbard model at half-filling. In particular, we will assess the evolution of the Fermi surface by varying the Coulomb interaction. In the insulating state, the underlying Fermi surface is given by the boundary of the occupied states of the renormalized dispersion relation, when the residual interactions giving rise to the charge gap are turned off in a Gedanken experiment.⁵⁻⁹ Mathematically, the underlying Fermi surface is defined in a non-Fermi-liquid state as the locus in k space where the real part of the one-particle Green's function changes its sign.^{5,10} By investigating magnetic and charge properties, we find that the Fermi surface reconstructs in a first-order manner right at the Mott transition. In particular, the Fermi surface is generic, namely, non-nesting, in the metallic side, whereas it has perfect nesting properties in the insulating state, at the transition point.

The paper is organized as follows: in Sec. II, we introduce the Hamiltonian; in Sec. III, we describe our variational wave function; in Sec. IV, we present our numerical results and, finally, in Sec. V we draw the conclusions.

II. MODEL

We consider the one-dimensional t_1 - t_2 Hubbard model

$$\mathcal{H} = - \sum_{i,\sigma,n=1,2} t_n c_{i,\sigma}^\dagger c_{i+n,\sigma} + \text{H.c.} + U \sum_i n_{i,\uparrow} n_{i,\downarrow}, \quad (1)$$

where $c_{i,\sigma}^\dagger$ is the electron creation operator, $\sigma = \uparrow, \downarrow$ the electron spin, $i = 1, \dots, L$ the site index, $n_{i,\sigma} = c_{i,\sigma}^\dagger c_{i,\sigma}$ the electron density, t_1 and t_2 the nearest and next-nearest neighbor hopping amplitudes,¹¹ and U the on-site Coulomb repulsion. In this work, we focus our attention on the half-filled case with L electrons on L sites.

The ground state of the t_1 - t_2 Hubbard model at half-filling is predicted to be an insulator with gapless spin excitations (conventionally labeled as C0S1) for $t_2/t_1 < 1/2$ and every finite U/t_1 ,¹² a spin-gapped metal (C1S0) with strong superconducting fluctuations for $t_2/t_1 > 1/2$ and small U/t_1 ,¹³ and a fully gapped spontaneously dimerized insulator (C0S0) for $t_2/t_1 > 1/2$ and large U/t_1 .^{14,15} Our findings, which are summarized in Fig. 1, are in very good agreement with these results. The locus of the metal-insulator transition has been investigated by several groups,¹⁶⁻¹⁹ with slightly varying outcomes. Remarkably, a transition between incommensurate and commensurate spin excitations is expected to take place inside the C0S0 phase.^{15,18,20} Finally, we would like to mention that a tiny C2S2 phase could be stable for $U/t_1 \rightarrow 0$, as suggested by a weak-coupling renormalization group approach;²¹ recent calculations showed that this phase can be further stabilized in presence of long-range interactions.²²

III. VARIATIONAL APPROACH

In this paper, we present a variational Monte Carlo study of the Hubbard model for $t_2/t_1 > 1/2$, which allows us to determine accurately the locus of the metal-insulator transition, to study the transition between commensurate and incommensurate spin-spin correlations in the large- U (dimerized) phase and to investigate its underlying Fermi surface. In particular, we will show that the magnetic correlations are related to the single-particle spectrum in the optimized variational wave function. Moreover, we will propose that the metal-insulator transition is driven in the Mott state by a

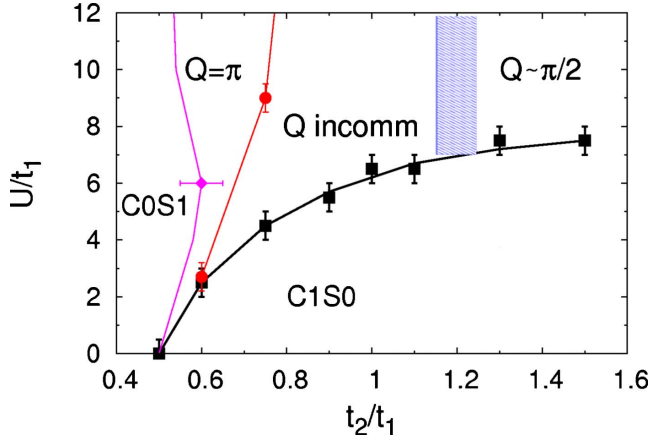


FIG. 1. (Color online) Phase diagram of the t_1 - t_2 Hubbard model at half-filling with the metallic phase with gapped spin excitations (C1S0) and the insulating phase with gapless spin excitations (C0S1). The insulating phase with gapped spin excitations for larger U and $t_2/t_1 > 1/2$ has regions with commensurate ($Q=\pi$) and incommensurate (Q incomm) spin-spin correlations. A crossover region separates the phase where the peak in $S(q)$ is incommensurate and the one with the peak commensurate to a doubled unit cell ($Q \sim \pi/2$).

renormalization of the underlying Fermi surface to perfect nesting.

Both the metallic and the insulating phases can be constructed, in a variational approach. In a first step, one constructs uncorrelated wave functions given by the ground state $|\text{BCS}\rangle$ of a superconducting Bardeen-Cooper-Schrieffer (BCS) Hamiltonian,^{23,24}

$$\mathcal{H}_{\text{BCS}} = \sum_{q,\sigma} \epsilon_q c_{q,\sigma}^\dagger c_{q,\sigma} + \sum_q \Delta_q c_{q,\uparrow}^\dagger c_{-q,\downarrow}^\dagger + \text{H.c.}, \quad (2)$$

where both the free-band dispersion ϵ_q and the pairing amplitudes Δ_q are variational functions. We use the parametrization

$$\epsilon_q = -2\tilde{t}_1 \cos q - 2\tilde{t}_2 \cos(2q) - \mu,$$

$$\Delta_q = \Delta_1 \cos q + \Delta_2 \cos(2q) + \Delta_3 \cos(3q), \quad (3)$$

where the effective hopping amplitudes \tilde{t}_1 and \tilde{t}_2 , as well as the effective chemical potential μ and the local pairing fields Δ_1 , Δ_2 , and Δ_3 are variational parameters to be optimized. The excitation spectrum for Bogoliubov excitations is given by

$$E_q = \sqrt{\epsilon_q^2 + \Delta_q^2}. \quad (4)$$

The correlated state $|\Psi_{\text{BCS}}\rangle$ is then given by

$$|\Psi_{\text{BCS}}\rangle = \mathcal{J}|\text{BCS}\rangle, \quad (5)$$

where $\mathcal{J} = \exp(-1/2 \sum_{i,j} v_{i,j} n_i n_j)$ is a density-density Jastrow factor (including the on-site Gutzwiller term), with the $v_{i,j}$ being optimized independently for every distance $|i-j|$. Notably, within this kind of wave function, it is possible to obtain a pure (i.e., nonmagnetic) Mott insulator by considering a sufficiently strong Jastrow factor,²⁵ i.e., $v_q \sim 1/q^2$ (v_q being

the Fourier transform of $v_{i,j}$) and a Luttinger-liquid wave function with arbitrary critical exponents,²⁶ whenever $v_{i,j} \sim \log|i-j|$. In addition, a dimerized phase can be obtained just by considering a gapped BCS spectrum E_q together with $v_q \sim 1/q^2$ (that is the case whenever $t_2/t_1 > 1/2$ and U/t_1 is large enough).²⁵ Remarkably, in this case, finite dimer-dimer correlations are found at large distance, even though the wave function does not break the translational symmetry. Here, we do not report results on dimer-dimer correlations, that are found in the C0S0 phase (see Ref. 25), but we concentrate on spin and charge properties, with a particular emphasis on the evolution of the Fermi surface by changing t_2/t_1 and U/t_1 .

As we demonstrated recently,²⁷ the projected BCS state $|\Psi_{\text{BCS}}\rangle$ can be improved further by considering backflow correlations, which modify the single-particle orbitals, in the same spirit as proposed by Feynman and Cohen.²⁸ In this way, already the determinant part of the wave function includes now correlation effects. All results presented here are obtained by fully incorporating the backflow corrections and optimizing individually every variational parameter in ϵ_q and Δ_q of Eq. (3), in the Jastrow factor \mathcal{J} of Eq. (5), as well as backflow corrections.

IV. RESULTS

A. Mott-Hubbard transition

The ground-state properties can be easily assessed by computing density and magnetic structure factors

$$N(q) = \frac{1}{L} \sum_{k,l} e^{iq(k-l)} \langle n_k n_l \rangle, \quad (6)$$

$$S(q) = \frac{1}{L} \sum_{k,l} e^{iq(k-l)} \langle S_k^z S_l^z \rangle, \quad (7)$$

where n_k and S_k^z are the total density and the z component of the spin operator on-site k , respectively.

The static density-density correlations behave qualitatively different in a metallic and a Mott-insulating state for small momenta q , with the metallic state being characterized by a linear dependence of $N(q) \sim q$, while in the insulating phase $N(q) \sim q^2$.²⁵ In Fig. 2, we present the behavior of $N(q)/q$ across the transition for three values of the ratio t_2/t_1 . The locus of the Mott-Hubbard transition can be determined easily, allowing us to draw the phase diagram in Fig. 1. Our determination of the line separating the metallic and the insulating phase is in good agreement with Refs. 16 and 18.

The metallic region in the phase diagram can be described as a Luther-Emery liquid, with a finite gap in the spin excitation spectrum and gapless charge excitations.²⁹ The charge stiffness K_ρ can be extracted, for example, from the long-distance behavior of the density-density correlations. In any conducting phase, we expect that K_ρ is also related to the slope of $N(q)$ at small q , i.e., $N(q) \sim K_\rho |q| / \pi$. In fact, the latter equation, which is definitely valid in Luttinger liquids, should hold whenever the charge degrees of freedom are gapless.²⁹ This procedure to obtain K_ρ works very well for

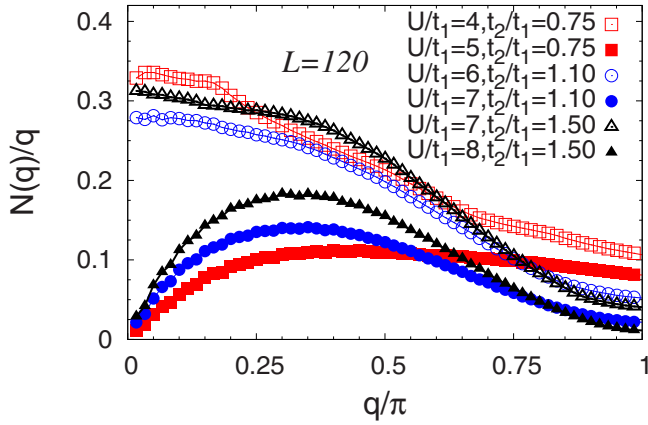


FIG. 2. (Color online) For a chain with $L=120$ sites, the density-density correlations $N(q)$, divided by the momentum q , across the metal-insulator transition for $t_2/t_1=0.75, 1.1$, and 1.5 . The metallic (insulating) state is characterized by a finite (vanishing) value of $N(q)/q$, in the limit $q \rightarrow 0$.

the doped single-band Hubbard model, namely, for the model of Eq. (1) with $t_2=0$,³⁰ in comparison with the exact results, as obtained by Bethe ansatz.³¹ By using $N(q)=2K_\rho|q|/\pi$, we obtain that $K_\rho \rightarrow 1$ for $U/t \rightarrow 0$ and $K_\rho \rightarrow 1/2$ at the metal-insulator transition.

B. Magnetic properties

The presence of *short-range* magnetic order is signaled by the appearance of a peak in $S(q)$, for a certain momentum Q . In the following, we will compare the magnetic properties with the renormalized single-particle spectrum E_q of the optimized variational wave function. The energy scale for E_q will be taken as the bandwidth W of the original free dispersion $\epsilon_q^0 = -2t_1 \cos(q) - 2t_2 \cos(2q)$. Note that, in the noninteracting case, there is only a single, perfectly nested Fermi surface for $t_2/t_1 < 0.5$, with two Fermi points separated by π . Instead, for $t_2/t_1 > 0.5$ there are two Fermi seas and four Fermi points.

In the metallic phase, the spin properties are only slightly modified by the presence of a small but finite interaction U , with respect to the $U=0$ behavior; for $t_2/t_1 > 0.5$ the single-particle spectrum E_q exhibits four minima, at $\pm k_1$ and $\pm k_2$, and the peak of $S(q)$ is located at $Q^{\text{met}} = k_2 - k_1 = \pi/2$. The condition $Q^{\text{met}} = \pi/2$ is determined by the Luttinger sum rule for the metal, which states that the total volume of the Fermi sea equals the number of electrons. In the insulating phase, the situation changes qualitatively and the magnetic properties of the system become strongly affected by the value of t_2/t_1 .

In Fig. 3, we show the behavior of $S(q)$ across the metal-insulator transition for $t_2/t_1=0.75$, in comparison with the variationally determined renormalized single-particle spectrum E_q . It can be observed that, when entering the insulating phase, the single-particle spectrum becomes strongly gapped and the two central minima collapse into a unique relative minimum at $q=0$, that subsequently disappears, as U/t_1 increases. At the same time, the peak in $S(q)$ shifts from $Q^{\text{met}} = \pi/2$ to $Q^{\text{ins}} = \pi$. Remarkably, just above the Mott tran-

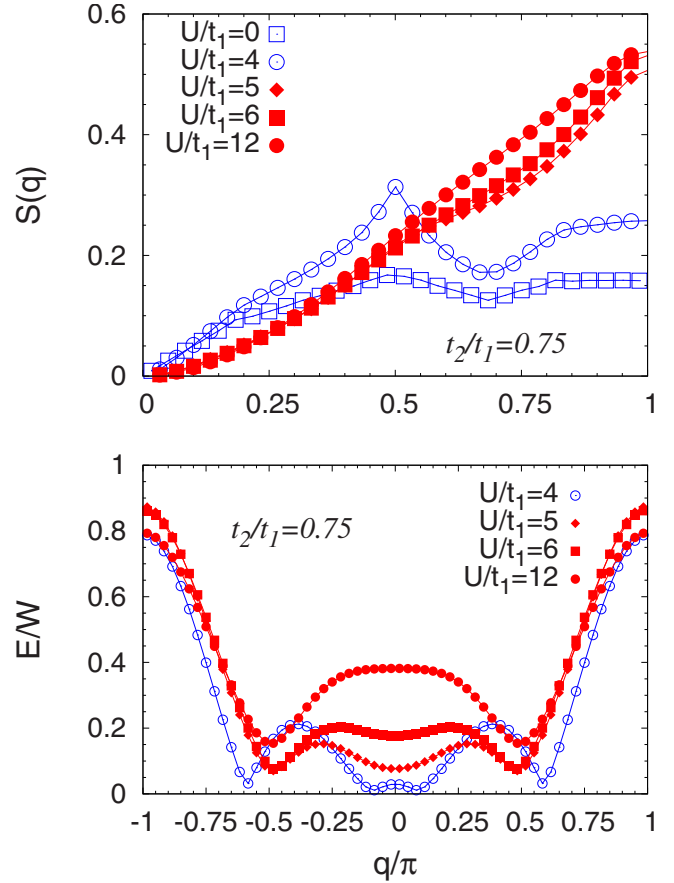


FIG. 3. (Color online) Upper panel: spin-spin correlations $S(q)$ at $t_2/t_1=0.75$, for a $L=120$ chain. Data are shown for $U/t_1=0, 4$ (metal) and for $U/t_1=5, 6, 12$ (insulator). Lower panel: single-particle spectrum E_q/W at $t_2/t_1=0.75$ for the same values of the electron-electron repulsion U and the same chain length.

sition, namely, for $5 < U/t_1 < 10$, the quantity $2k_1$ (i.e., the distance between the two absolute minima of E_q) is slightly different from π and becomes commensurate only after a second transition (e.g., $U/t_1 \approx 9$), inside the insulating phase,¹⁸ see Fig. 4. However, the degree of incommensurability is very small and does not show up in corresponding

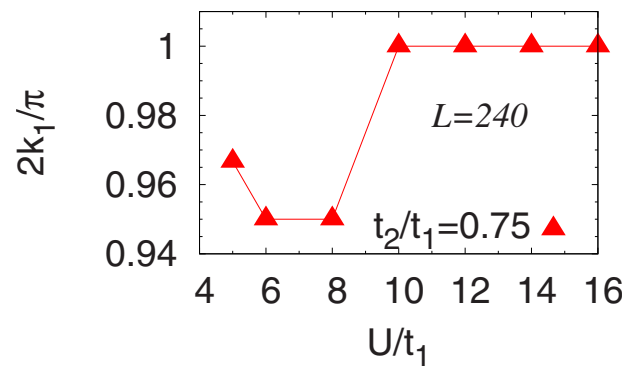


FIG. 4. (Color online) Evolution of $2k_1$ (distance between the minima of the single-particle spectrum E_q) in the insulating phase for $t_2/t_1=0.75$. Note the transition from an incommensurate to a commensurate value for $U/t_1 \approx 9$.

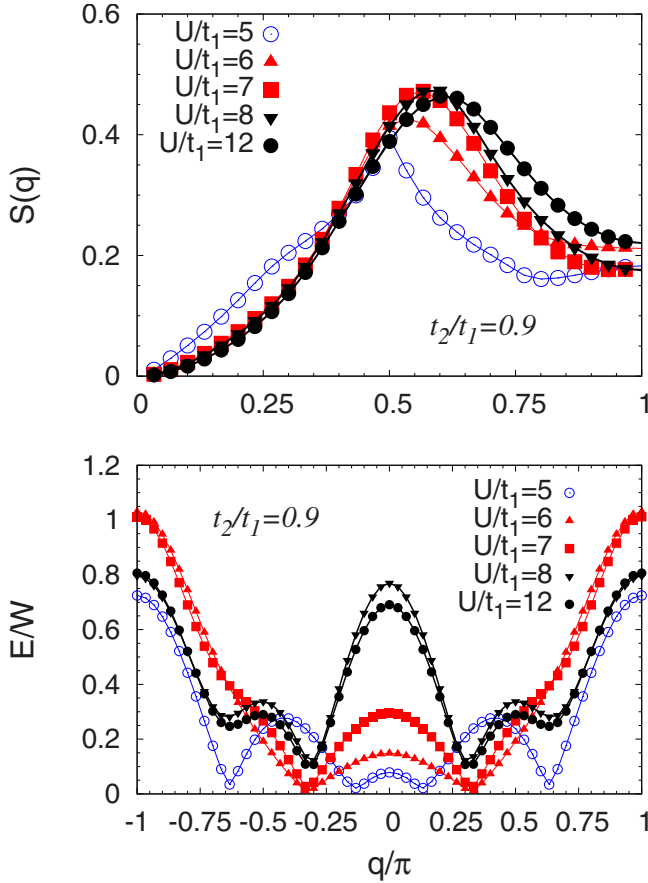


FIG. 5. (Color online) Upper panel: spin-spin correlations $S(q)$ at $t_2/t_1=0.9$, for a $L=120$ chain. Data are shown for $U/t_1=5$ (metal) and $U/t_1=6,7,8,12$ (insulator). Lower panel: single-particle spectrum E_q/W at $t_2/t_1=0.9$ for the same values of the electron-electron repulsion U and the same chain length.

shift in the peak in $S(q)$ from $Q^{\text{ins}} = \pi$. Indeed, the magnetic correlations are short-ranged and the peak in $S(q)$ is consequently broad. A shift in the momentum away from π will therefore result in a shift in the maximum in $S(q)$ only for a substantial degree of incommensurability.

In Fig. 5, we plot the spin-spin correlations $S(q)$ and the single-particle spectrum E_q for the ratio $t_2/t_1=0.9$. In the metallic phase, the spin-spin correlations are always peaked at $Q^{\text{met}} = \pi/2$, while in the insulating phase the peak slowly shifts to $Q \approx 0.6\pi$. For $U=6$ and 7 the single-particle spectrum E_q is qualitatively different from the one for larger U 's. As shown later, this is related to the different behavior of the variational hopping ratio \tilde{t}_2/\tilde{t}_1 close to the metal-insulator transition with respect to the strong-coupling regime. For larger values of the ratio U/t_1 , E_q shows four local minima, with the peak in $S(q)$ located at $Q^{\text{ins}} = 2k_1$, where $2k_1$ is the distance between the two absolute minima.

Finally, in Fig. 6, we summarize the spin-spin correlations for different t_2/t_1 , at a given value of U/t_1 , chosen to be far enough from the metal-insulator transition in order to describe the large- U behavior of $S(q)$. The peak in the spin-spin correlations exhibits the commensurate-incommensurate transition moving far from $Q = \pi$, as the ratio t_2/t_1 is increased. When $t_2/t_1=1.5$ the system behaves already like in

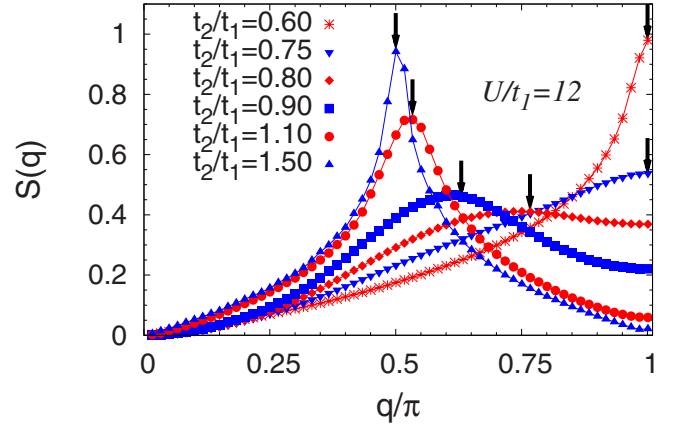


FIG. 6. (Color online) The spin-spin correlations $S(q)$ at $U/t_1=12$ and for $L=120$ sites, for different values of the hopping ratio t_2/t_1 . Arrows indicate the quantity $2k_1$, obtained from the single-particle spectrum E_q .

the $t_2/t_1 \rightarrow \infty$ limit, with the peak commensurate to a lattice with a doubled unit cell ($Q = \pi/2$). These results are in agreement with previous studies for the Heisenberg³² and the Hubbard model.¹⁵

C. Fermi-surface renormalization

Finally, we present our central result, namely, the fact that the metal-insulator transition is driven, in the Mott-insulating state, by a renormalization of the underlying Fermi surface to perfect nesting. With underlying Fermi surface, we mean the locus of the highest occupied momenta in the noninteracting spectrum $\epsilon_q = -2\tilde{t}_1 \cos(q) - 2\tilde{t}_2 \cos(2q)$, obtained from the optimized variational hopping parameters. We would like to stress that the concept of an underlying Fermi surface is of central importance for the angular resolved photoemission spectroscopy (ARPES) studies of strongly correlated systems, like the high-temperature superconductors.⁵⁻⁸ Note, that $E_q = \sqrt{\epsilon_q^2 + \Delta_q^2}$ corresponds within renormalized mean-field theory²⁴ to the excitation spectrum of projected Bogoliubov quasiparticles and ϵ_q hence to the dispersion of the renormalized quasiparticles. Moreover, recent calculations on the t - J and the periodic Anderson models highlighted the possibility to assess the Fermi surface from the parametrization of a variational wave function.^{33,34} Here, the renormalization of the hopping parameters made it possible to show nontrivial deformations of the noninteracting Fermi surface, due to the Gutzwiller projection.

We show in Fig. 7 that the ratio \tilde{t}_2/\tilde{t}_1 in the metallic phase is almost equal to the bare value t_2/t_1 , regardless of the degree of interaction. This weak renormalization of the band structure in the metallic state is in agreement with a renormalization-group study,²¹ which predicts that the renormalization of the Fermi surface is proportional to U^2 . Then, after the metal-insulator transition, the ratio jumps to a smaller value, very close to $1/2$. According to our data, we propose that the optimized variational ratio of \tilde{t}_2/\tilde{t}_1 is renormalized to $1/2$, exactly at the metal-insulator transition. This discontinuous behavior of the renormalized band structure is

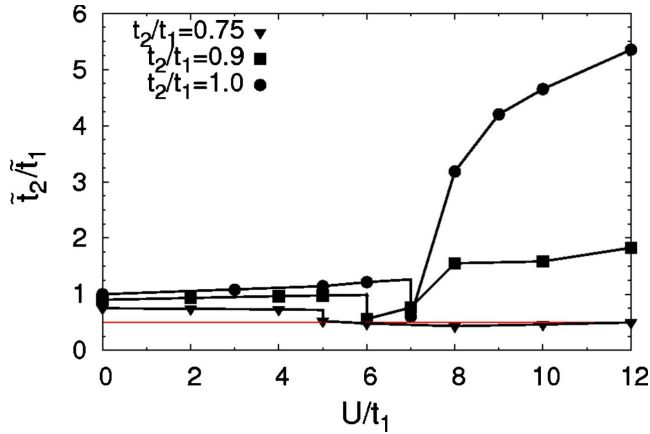


FIG. 7. (Color online) The variationally optimized hopping ratio \tilde{t}_2/\tilde{t}_1 in |BCS>, see Eq. (5), as a function of U/t_1 . The metal-insulator transition takes place for $U/t_1 = 4.5 \pm 0.5$, 5.5 ± 0.5 , and 6.5 ± 0.5 for $t_2/t_1 = 0.75$ (triangles), 0.9 (squares), and 1.0 (circles), respectively. The variational state |BCS> contains only a single Fermi sea for $\tilde{t}_2/\tilde{t}_1 \leq 0.5$ (horizontal line).

also evident in Fig. 5, e.g., for $t_2/t_1 = 0.9$, with the number of minima of the single-particle spectrum E_q jumping from four to two when entering the Mott-insulating state. We note that an analogous tendency toward a Fermi-surface symmetrization in the insulating state has been observed in a study of a two-dimensional frustrated lattice.^{35,36}

A renormalization of the variational hopping ratio to $\tilde{t}_2/\tilde{t}_1 = 1/2$ implies that the Fermi surface is nested, with two Fermi points separated by a vector π . This perfect nesting condition drives the system to be an insulator, generating a charge gap as soon as electron-electron interaction is switched on. Remarkably, while the metal-insulator transition is driven by the renormalized dispersion ϵ_q , the pairing terms Δ_q are crucial in determining the spin properties of the

model, via the renormalized excitation spectra $E_q = \sqrt{\epsilon_q^2 + \Delta_q^2}$. Indeed, as shown, for example, in Fig. 5, the minima of the single-particle spectrum at $t_2/t_1 = 0.9$ are connected by an incommensurate vector, leading to an incommensurate peak in $S(q)$.

V. CONCLUSIONS

We have presented an extensive study of the phase diagram of the one-dimensional t_1-t_2 Hubbard model at half-filling, with emphasis on the evolution of the magnetic properties and of the underlying Fermi surface across the interaction-driven Mott-Hubbard transition. We have shown that the magnetic correlations are related to the single-particle spectrum in the optimized variational wave function and we have described how they are affected by the metal-insulator transition. In the insulating phase, the peak in the spin-spin correlations exhibits the commensurate-incommensurate transition moving far from $Q = \pi$, as the ratio t_2/t_1 is increased, and then becomes commensurate to a doubled unit cell when $t_2/t_1 \geq 1.3$.

Our main findings culminate in the hypothesis that the underlying Fermi surface renormalizes to perfect nesting right at the transition in the insulating phase, with a first-order reorganization when crossing the transition into the metallic state. Similar renormalizations of the Fermi surface have been observed in two-dimensional models.^{5,35,36} Therefore, we believe that our results are important for an improved understanding of Mott-Hubbard transitions quite in general, transcending the specific one-dimensional physics.

ACKNOWLEDGMENT

L.F.T. and C.G. acknowledge the support of the German Science Foundation through the Transregio 49.

¹N. Toyota, M. Lang, and J. Müller, *Low-Dimensional Molecular Metals* (Springer, New York, 2007).

²S. Giorgini, L. P. Pitaevskii, and S. Stringari, *Rev. Mod. Phys.* **80**, 1215 (2008).

³I. Shinichiro and H. Okamoto, *J. Phys. Soc. Jpn.* **75**, 011007 (2006).

⁴H. Kishida, H. Matsuzaki, H. Okamoto, T. Manabe, M. Yamashita, Y. Taguchi, and Y. Tokura, *Nature (London)* **405**, 929 (2000).

⁵C. Gros, B. Edegger, V. N. Muthukumar, and P. W. Anderson, *Proc. Natl. Acad. Sci. U.S.A.* **103**, 14298 (2006).

⁶T. Yoshida, X. J. Zhou, K. Tanaka, W. L. Yang, Z. Hussain, Z.-X. Shen, A. Fujimori, S. Sahrakorpi, M. Lindroos, R. S. Markiewicz, A. Bansil, Seiki Komiyama, Yoichi Ando, H. Eisaki, T. Kakeshita, and S. Uchida, *Phys. Rev. B* **74**, 224510 (2006).

⁷B. Edegger, V. N. Muthukumar, and C. Gros, *Adv. Phys.* **56**, 927 (2007).

⁸R. Sensarma, M. Randeria, and N. Trivedi, *Phys. Rev. Lett.* **98**, 027004 (2007).

⁹J. Kokalj and P. Prelovsek, *Phys. Rev. B* **75**, 045111 (2007); **78**, 153103 (2008).

¹⁰I. Dzyaloshinskii, *Phys. Rev. B* **68**, 085113 (2003).

¹¹At half-filling the relative sign between t_1 and t_2 is irrelevant.

¹²E. H. Lieb and F. Y. Wu, *Phys. Rev. Lett.* **20**, 1445 (1968).

¹³M. Fabrizio, *Phys. Rev. B* **54**, 10054 (1996).

¹⁴R. Arita, K. Kuroki, H. Aoki, and M. Fabrizio, *Phys. Rev. B* **57**, 10324 (1998).

¹⁵S. Daul and R. M. Noack, *Phys. Rev. B* **61**, 1646 (2000).

¹⁶M. E. Torio, A. A. Aligia, and H. A. Ceccatto, *Phys. Rev. B* **67**, 165102 (2003).

¹⁷C. Aebischer, D. Baeriswyl, and R. M. Noack, *Phys. Rev. Lett.* **86**, 468 (2001).

¹⁸C. Gros, K. Hamacher, and W. Wenzel, *EPL* **69**, 616 (2005).

¹⁹G. I. Japaridze, R. M. Noack, D. Baeriswyl, and L. Tincani, *Phys. Rev. B* **76**, 115118 (2007).

²⁰C. Berthod, T. Giamarchi, S. Biermann, and A. Georges, *Phys. Rev. Lett.* **97**, 136401 (2006).

²¹K. Louis, J. V. Alvarez, and C. Gros, *Phys. Rev. B* **64**, 113106

- (2001).
- ²²H.-H. Lai and O. I. Motrunich, *Phys. Rev. B* **81**, 045105 (2010).
- ²³C. Gros, *Phys. Rev. B* **38**, 931(R) (1988).
- ²⁴F. C. Zhang, C. Gros, T. M. Rice, and H. Shiba, *Supercond. Sci. Technol.* **1**, 36 (1988).
- ²⁵M. Capello, F. Becca, M. Fabrizio, S. Sorella, and E. Tosatti, *Phys. Rev. Lett.* **94**, 026406 (2005).
- ²⁶C. S. Hellberg and E. J. Mele, *Phys. Rev. Lett.* **67**, 2080 (1991); R. Valentí and C. Gros, *ibid.* **68**, 2402 (1992).
- ²⁷L. F. Tocchio, F. Becca, A. Parola, and S. Sorella, *Phys. Rev. B* **78**, 041101(R) (2008).
- ²⁸R. P. Feynman and M. Cohen, *Phys. Rev.* **102**, 1189 (1956).
- ²⁹J. Solyom, *Adv. Phys.* **28**, 201 (1979).
- ³⁰M. Capello, F. Becca, S. Yunoki, M. Fabrizio, and S. Sorella, *Phys. Rev. B* **72**, 085121 (2005).
- ³¹H. J. Schulz, *Int. J. Mod. Phys. B* **5**, 57 (1991).
- ³²R. Bursill, G. A. Gehring, D. J. J. Farnell, J. B. Parkinson, T. Xiang, and C. Zeng, *J. Phys.: Condens. Matter* **7**, 8605 (1995).
- ³³A. Himeda and M. Ogata, *Phys. Rev. Lett.* **85**, 4345 (2000).
- ³⁴H. Watanabe and M. Ogata, *Phys. Rev. Lett.* **99**, 136401 (2007); *J. Phys. Soc. Jpn.* **78**, 024715 (2009).
- ³⁵J. Liu, J. Schmalian, and N. Trivedi, *Phys. Rev. Lett.* **94**, 127003 (2005).
- ³⁶L. F. Tocchio, A. Parola, C. Gros, and F. Becca, *Phys. Rev. B* **80**, 064419 (2009).